COMMUNICATIONS EARTH&ENVIRONMENT

ARTICLE

https://doi.org/10.1038/s43247-020-00016-3 OPEN

A quantitative hydroclimatic context for the European Great Famine of 1315–1317

Seung H. Baek[1,2✉], Jason E. Smerdon[1], George-Costin Dobrin[3], Jacob G. Naimark[3], Edward R. Cook[1], Benjamin I. Cook[1,4], Richard Seager[1], Mark A. Cane[1] & Serena R. Scholz[5]

The European Great Famine of 1315–1317 triggered one of the worst population collapses in European history and ranks as the single worst European famine in mortality as a proportion of population. Historical records point to torrential rainfall, land saturation, crop failure, and prolonged flooding as important causes of the famine. Here we use the tree-ring based Old World Drought Atlas (OWDA) to show that the average of each growing season preceding the Great Famine years (1314–1316) was the fifth wettest over Europe from 1300 to 2012 C.E. The spatial and temporal characteristics of our OWDA-estimated anomalies are in excellent agreement with available historical accounts. We also characterize a mode of European hydroclimate variability that is associated with the Great Famine, which we term the "Great Famine mode." This mode emerges as the leading mode of European hydroclimate variability from 1300–2012 and is strongly associated with extreme wet and dry events in Europe over the last millennium.

[1] Lamont-Doherty Earth Observatory, Columbia University, Palisades, NY, USA. [2] Department of Earth and Environmental Sciences, Columbia University, New York, NY, USA. [3] Columbia College, Columbia University, New York, NY, USA. [4] NASA Goddard Institute for Space Studies, New York, NY, USA. [5] Department of Earth and Environmental Sciences, University of Michigan, Ann Arbor, MI, USA. ✉email: sbaek@ldeo.columbia.edu

Death by war, famine, and disease were common in Medieval Europe, but the sheer volume of lives lost in the 14th century stands out, marked by such infamous events as the Hundred Years' War[1] and the Black Death[2]. The European Great Famine of 1315–1317, the first catastrophic event of the century, starved millions across Europe. It was closely linked to climatic drivers[3], coinciding with cooler summers[4] during the transition of the Northern Hemisphere from the Medieval Warm Period (~950–1250 C.E.[5]) to the Little Ice Age (~1450–1850[5]), but most directly tied to a prolonged period of prodigious precipitation that began as early as 1314 and continued into 1316[6]. The rain was described as an "incessant downpour, day and night, in most miraculous fashion such as no mortal then living had ever seen," the likes of which were compared to the fulfillment of the Noah's Ark prophecy[6]. The rain caused widespread agricultural failures which in turn led to near unprecedented levels of famine that continued in some locations until 1321 or 1322[7,8]. Wheat prices in England rose from five shillings in 1313 to up to forty shillings by 1315, and hunger was so acute in Poland and Silesia that cannibalism and infanticide were reported among the peasantry[6]. One memorial stone at the Church of Schmidtstedt, Germany, commemorates the terrible loses in just one community alone: "In the year of the Lord 1316 here were buried 100 × 60, 33 × 60, and 5 [7985] humans, who have died in the years of dearness. God have mercy on them[9]."

Despite the Great Famine's status as the most notorious and chronicled of all medieval famines[6–8,10,11], historical evidence of the hydroclimate conditions remains almost exclusively qualitative. A brief but more quantitative paleoclimatic assessment of the Great Famine was provided by Cook et al.[12] in their release of the Old-World Drought Atlas (OWDA), which is a tree-ring derived paleoclimatic product that estimates soil moisture conditions over Europe during boreal summer (June–July–August) by calibrating on the self-calibrating Palmer Drought Severity Index (scPDSI;[13] see Methods section). Here we examine in greater detail the OWDA and its spatiotemporal estimates of normalized soil moisture during the Great Famine.

Results

Hydroclimatic conditions of the Great Famine. Positive and negative scPDSI values of a given grid point indicate that soil moisture is wetter or drier than normal, respectively, for that locality, with values for scPDSI typically falling between +4 (extremely wet) and −4 (extremely dry). Consistent with Cook et al.[12], the OWDA shows extremely wet summer conditions over much of Europe in 1314–1316, the three years preceding the canonical famine period of 1315–1317 (Fig. 1), with the wetness centered over modern-day France, Ireland, the United Kingdom, Belgium, Switzerland, Germany, Denmark, Poland, Lithuania, Latvia, and Estonia. A cohesive pattern of widespread wetness persists for each summer in 1314, 1315, and 1316, with many regions reaching scPDSI values in the +4 to +6 range, before dissipating to more neutral conditions over much of the domain in 1317.

We contextualize these wet conditions over the last millennium by ranking the 1314, 1315, and 1316 summers in each grid point by wetness relative to all summers from 1300 to 2012. In 1314, only regions in France, the United Kingdom, and Finland rank among the wettest in the last millennium. By 1315 and 1316, however, almost all of Europe ranks among the wettest summers over the analysis period, with many regions ranking in the top 10. The 1314–1316 summer mean furthermore comprises the fifth wettest 3-year summer period over Europe from 1300 to 2012. Three of the four other 3-year summer periods ranked higher than the Great Famine occur after 1710 when technology began to decouple climate shocks and famine[14]. The remaining 3-year summer period occurs in the late 14th century after the Black Death reduced the population to levels in which widespread famines were unlikely[2]. While the specific rank of the Great Famine summers is subject to reconstruction uncertainties, the 1314–1316 summer period is nevertheless in the top 1% of all 3-year summer periods in the 1300–2012 interval.

A ranking of wetness by country from 1300 to 2012 yields similar results (Table 1). For instance, the United Kingdom, France, Switzerland, and Belgium had average scPDSI values that

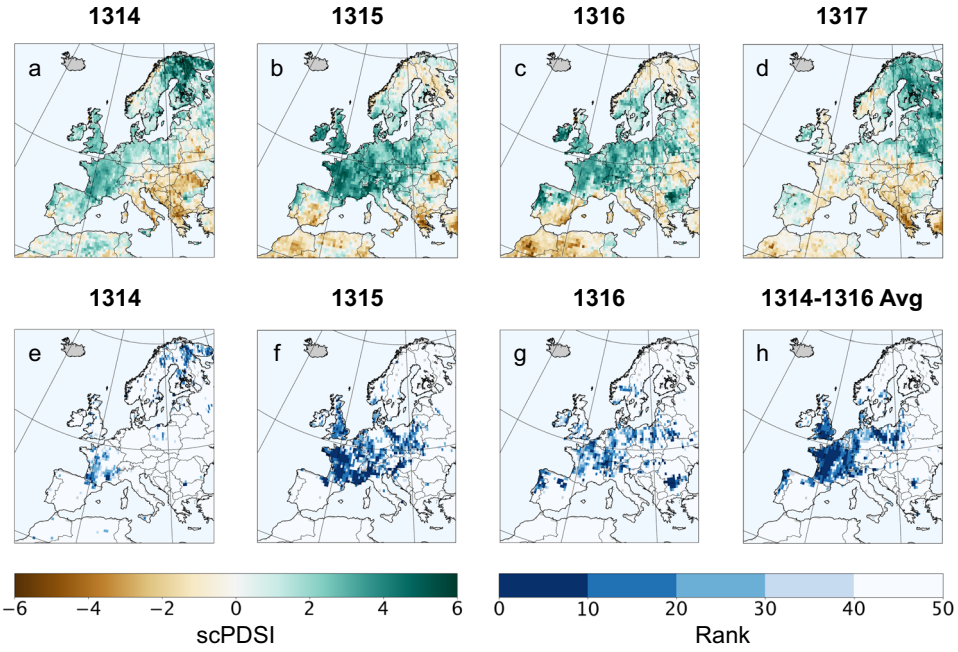

Fig. 1 The Great Famine years composited and ranked. (**a**–**d**, left to right) scPDSI values for the years **a** 1314, **b** 1315, **c** 1316, and **d** 1317. (**e**–**f**, left to right) The scPDSI rank at each grid point for the **e** 1314, **f** 1315, **g** 1316 years individually, and for the **h** 1314–1316 3-year interval, all relative to 1300–2012. All locations with rankings below 50 have been left white.

Table 1 Wetness rankings during the Great Famine by country.

Country	1314	1315	1316	1317	1314–1316	*N*	1314[a]	1315	1316
	Wet rank, all years				3-Year rank	Wet rank, famine years only			
	1300–1710 (1300–2012)					1300–1710 (1300–2012)			
United Kingdom	22 (38)	6 (10)	26 (47)	169 (296)	3 (4)	22 (28)	1 (1)	1 (1)	4 (4)
France	14 (23)	4 (8)	35 (56)	218 (378)	2 (5)	20 (24)	1 (1)	1 (1)	3 (3)
Germany	70 (124)	8 (17)	5 (13)	116 (201)	6 (14)	49 (83)	4 (5)	3 (4)	1 (2)
Switzerland	51 (92)	2 (6)	4 (12)	109 (189)	1 (6)	49 (83)	4 (5)	1 (2)	3 (4)
Austria	320 (552)	7 (18)	35 (65)	228 (407)	48 (89)	49 (83)	12 (23)	2 (4)	8 (12)
Belgium	37 (68)	5 (11)	34 (65)	238 (416)	4 (9)	40 (57)	3 (3)	1 (1)	4 (4)
Netherlands	62 (109)	9 (19)	29 (52)	190 (342)	8 (19)	40 (57)	3 (4)	1 (1)	4 (4)
Luxembourg	15 (32)	8 (19)	20 (40)	191 (336)	1 (7)	40 (57)	2 (2)	1 (1)	3 (3)
Italy[b]	299 (515)	44 (86)	237 (403)	362 (615)	174 (302)	52 (60)	41 (48)	9 (11)	33 (39)
All Countries[c]	18 (29)	2 (4)	23 (37)	197 (344)	2 (5)	76 (115)	2 (2)	1 (1)	5 (5)

[a]Compared to years preceding famines.
[b]Italy was not in famine for 1314, 1315, and 1316, but is provided a wet rank relative to famine years.
[c]Excluding Italy.
Rankings are over the 1300–1710 (1300–2012) periods. The wetness ranking for the 1314–1316 mean period and the wetness ranking for just famine years are also given.

rank 1315 in the top 10 wettest summers. For Europe as a whole (defined herein as "All Countries" listed in Table 1, which excludes Italy), 1315 was the 4th wettest summer. When 1314, 1315, and 1316 summers are ranked only relative to other summers during famines between 1300 and 2012[14], 1315 ranks as the wettest, while 1314 and 1316 are both in the top five.

Despite extreme rains during the Great Famine, climatological shock was often only the trigger for European famine, while overpopulation and social pressures were preconditioning for these events prior to 1710[14,15] (technological advances change this dependence post 1710[14]). For instance, population in England and France, the two countries impacted by the Great Famine with available population estimates during 1315–1317, were ~4.6 and ~16.7 million, respectively, levels that approached their estimated long-term maximum population capacities of 5 and 20 million, respectively[14] (see Table 2 for population ranking of England and France during the Great Famine). These population levels would have introduced population and associated social pressures on resources and created conditions favoring famine. Extreme rain may have thus struck upon this background of population pressure and social conditions, elevating the Great Famine to its status as a defining catastrophe of the Middle Ages.

The severity, timing, and geographical characteristics of our OWDA-estimated wet anomalies are in excellent agreement with available historical accounts summarized in comprehensive review articles (see refs. [6,8,10]). The torrential rains of 1315 are said to have begun in April and May over France and England, respectively[8,10]. In Grimma, Germany, the Mulde river swept away the church of the Austin Canons in 1315, while ruinous weather in the same year reached as far southeast as Salzburg, Austria; 1316 spring and summer rains are reported to have destroyed hay production and ruined the seeding in Poland and Hungary[6]. The Low Countries experienced perhaps the greatest rainfall in Europe, and there are reports of widespread late spring flooding in 1315[6]. Notably, significant scPDSI anomalies do not exist over southern Italy (Fig. 1 and Table 1), consistent with historical evidence chronicling southern Italy as one of the regions that exported food during the Great Famine[6]. Such excellent accord with existing historical evidence suggests that the OWDA can also provide insight where historical evidence is sparse, despite regions of heterogenous and sparse sampling that also exist within the underlying OWDA dataset (these sampling limitations are mitigated in part by the spatial covariance inherent to scPDSI and the OWDA reconstruction method). For instance, there is some uncertainty among historians whether the rain began in 1314 or 1315[6,8,16] and whether 1315 or 1316 was the wetter year[10]. Our estimates show that 1314 was a wet summer and that the 1315 summer was wetter than the 1316 summer over the majority of the impacted regions.

Table 2 Population rankings during the Great Famine for England and France.

Country	1314	1315	1316	1317	*N*	1314[a]	1315	1316	1317
	Population rank, all years 1300–1710				Population rank, famine years only				
England	109	110	114	119	22	4	4	5	6
France	259	252	248	244	50	12	18	17	15

[a]Compared to years preceding famines.
Rankings are relative to all years from 1300 to 1710 for England and France. Population rankings relative to only famine years during the 1300–1710 interval are also given.

The Great Famine mode. To further evaluate the nature of the Great Famine pattern, we perform an empirical orthogonal function (EOF) analysis of the OWDA from 1300 to 2012, decomposing the scPDSI field into orthogonal spatial covariance patterns and their respective temporal variability. We term the leading spatial covariance pattern, accounting for the greatest OWDA variance at 15%, as the "Great Famine mode" (GFM; Fig. 2). The nature and ordering of this mode are consistent with previous regression and EOF analyses of the OWDA[17], while we herein connect the mode to the Great Famine for the first time. Moving 3-year mean values of the temporal variability of the GFM correlate highly ($r = 0.95$) with moving 3-year spatially averaged European scPDSI values from 1300 to 2012 ($r = 0.94$ if correlations are calculated on yearly values). The 3-year averages, selected based on the relevant Great Famine window from 1314 to 1316, show that the GFM exerted broad influence across much of Europe; the wettest periods coincide with the largest values of the temporal variability associated with the GFM, with the 1314–1316 mean value ranking second highest from 1300 to 2012.

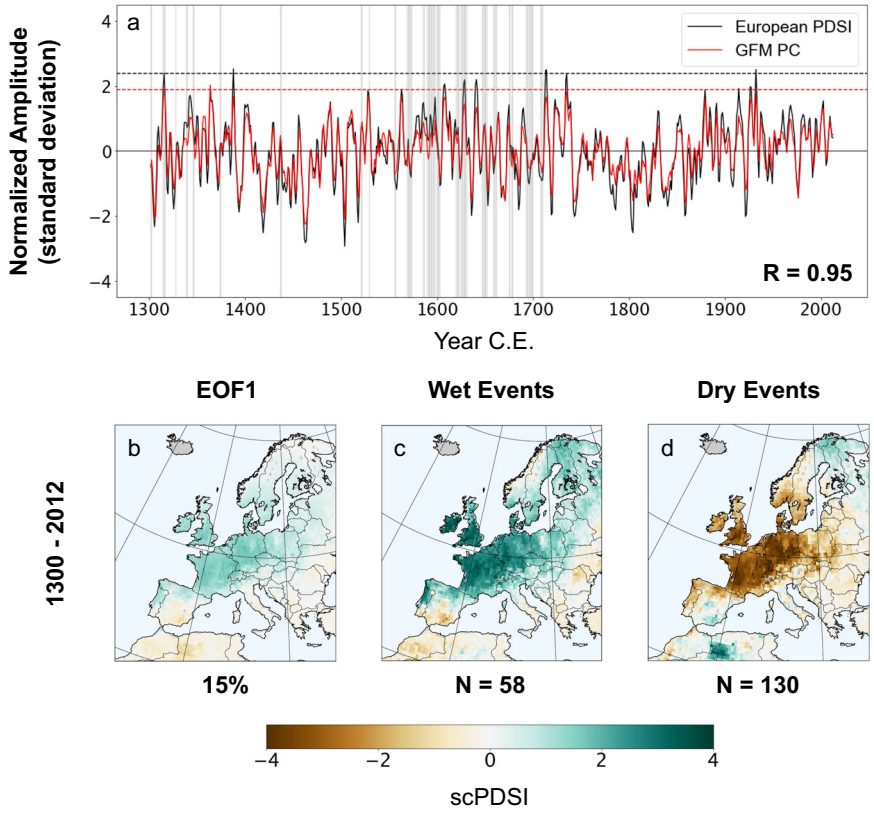

Fig. 2 The Great Famine and the Great Famine mode. a Three-year moving average of the principal component (PC) time series of the leading mode of variability over the OWDA, identified as the GFM, and 3-year moving average of scPDSI over Europe (defined as "All Countries," in Table 1, which excludes Italy) from 1300 to 2012 (both time series have been normalized to unit variance). Red (black) dashed line marks the normalized GFM PC (European scPDSI) value during the Great Famine years of 1314–1316. The Pearson's correlation coefficient between the GFM PC and scPDSI from 1300 to 2012 is provided in the lower right corner. Gray vertical lines mark famine years (identified only up to 1710). **b** The leading empirical orthogonal function (EOF) of the GFM in the OWDA from 1300 to 2012. The variance explained by the GFM is provided below the map. **c** Composite of the annual extreme wet anomalies from 1300 to 2012, defined as the years when the average scPDSI value over Europe is ≥1 ($N = 58$ years). **d** Composite of extreme dry anomaly years from 1300 to 2012, defined as the years when the average scPDSI value over Europe is ≤−1 ($N = 130$ years).

Moreover, the spatial pattern of the GFM is in strong agreement with the cohesive wet pattern in the OWDA in 1315 and 1316 (spatial correlations are $r = 0.71$ and $r = 0.68$, respectively) as well as the composite of the wettest scPDSI anomalies (scPDSI >1, $N = 58$ years) over Europe from 1300 to 2012 (spatial correlation $r = 0.85$). Conversely, the GFM is the inverse pattern of the composite of the driest scPDSI anomalies (spatial correlation $r = -0.88$) over the same interval (scPDSI <−1, $N = 130$ years). The GFM therefore not only exerted strong influences over Europe broadly, but is associated with the most extreme wet and dry hydroclimate anomalies over the last millennium, the Great Famine included.

Comparison of scPDSI and precipitation over Europe from 1901 to 2012 reveals the OWDA to be an excellent proxy for late spring/summer precipitation[18] (Fig. 3), the principal seasonal precipitation signal associated with the Great Famine. In both scPDSI and precipitation over the 1901–2012 period, the first leading mode is a predominantly North–South dipole mode (N–S mode), while the second leading mode appears as the GFM. The spatial patterns of the two leading modes in scPDSI compare well against those of the two leading modes in precipitation (spatial correlation $r = 0.75$ and 0.80, respectively); the variance explained by the two modes, at 15% and 12–13%, respectively, are also consistent. Moreover, the patterns in Fig. 3 are consistent with documented summer hydroclimate footprints over the observational interval[19,20], suggesting that the leading pattern expressed in the OWDA may be interpreted as the leading spring/summer precipitation pattern back to 1300.

Our identification of the GFM as the leading mode over 1300–2012 but not over the 20th century specifically suggests that the influence of the GFM associated with scPDSI, and likely precipitation, has waned in the 20th century relative to the last millennium. Variance of the GFM exceeds that of the N–S mode (identified as the second leading mode over 1300–2012) for most of the last millennium until ~1900 (Fig. 4), showing that although the GFM has been the leading mode of hydroclimate variability for most the last millennium, the 20th century has largely been free of extremes in GFM variability and is instead led by the N–S mode. This reordering of the leading mode in the OWDA during the 20th century indicates that the recent rise of the N–S mode has been anomalous. Moreover, the strong resemblance of the N–S mode to the canonical imprint of the winter North Atlantic Oscillation[21–26] (NAO), when considering that the OWDA carries memory of winter and early spring precipitation and soil moisture[18,27], additionally raises the question of whether the leading influence of the NAO on winter precipitation has been anomalous during the 20th century as well.

Discussion

The Great Famine was the result of a climatic shock that imprinted on existing population and social pressures. Here we

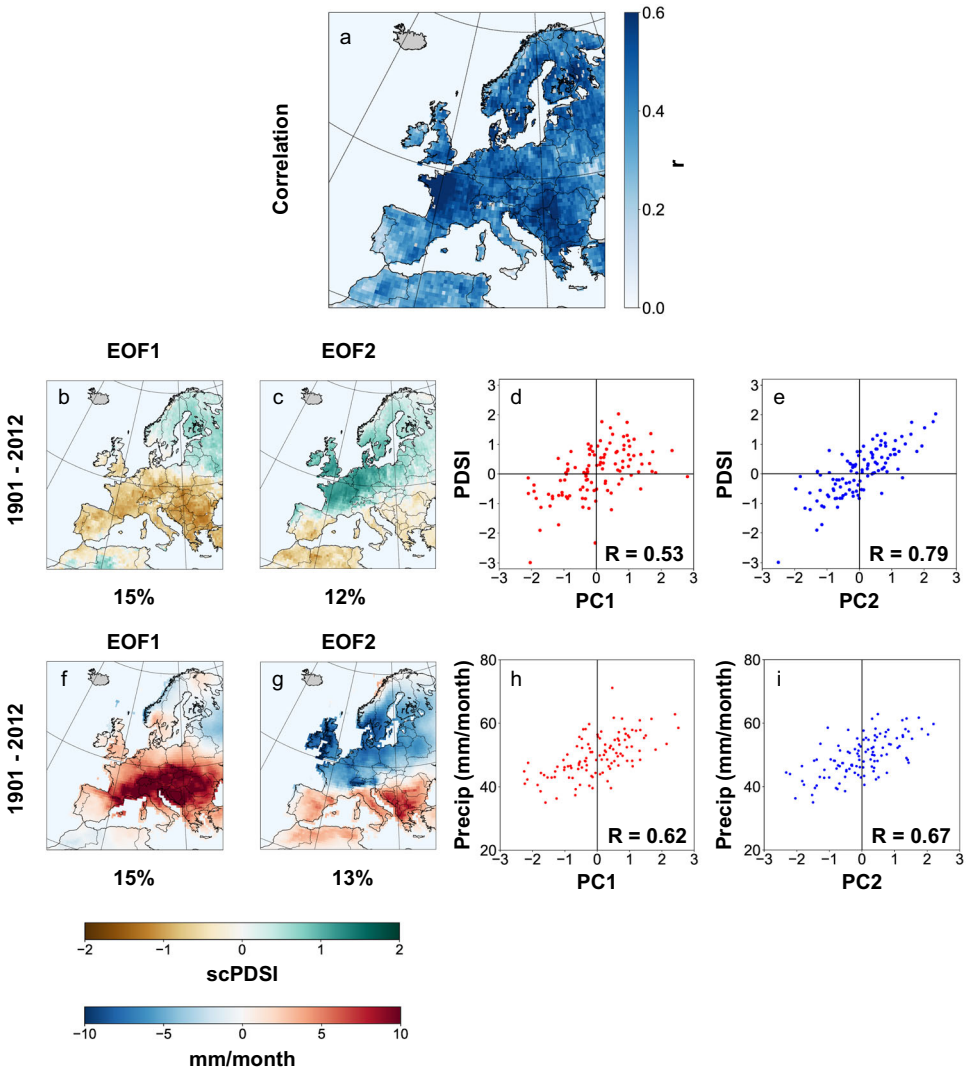

Fig. 3 Comparison of scPDSI and precipitation in relation to the Great Famine mode. a Correlations between co-located scPDSI and May–June–July (MJJ) precipitation over the OWDA domain from 1901 to 2012. Average correlation over the domain is maximized for these three months (not shown). (**b**, **c**, left to right) The **b** first and **c** second leading empirical orthogonal functions (EOFs) of the OWDA from 1901 to 2012. The variance explained by each mode is provided below the EOFs. (**d**, **e**, left to right) Scatter plots between the **d** first and **e** second principal component of the respective EOFs and average scPDSI over Europe (defined as "All Countries" in Table 1, which excludes Italy) from 1901 to 2012 (**f**–**i**). Same as **b**–**e**, but for 1901–2012 MJJ precipitation.

have explored in detail the climatological driver of the Great Famine, comparing tree-ring derived estimates of soil moisture conditions with numerous historical descriptions of the extreme rain. We find that the paleo-derived estimates of the temporal and geographical evolution of hydroclimate conditions during the Great Famine are in excellent agreement with historical accounts. Furthermore, our ranking of the Great Famine period as the 5th wettest 3-year interval over the last 700 years corroborates near-universal historical descriptions of the unusual nature of the rain at the time, while suggesting it was an event that truly stands out in a much longer historical context. We thus demonstrate that the OWDA can be a powerful complement to existing historical literature regarding the climatic triggers of the Great Famine. We have furthermore connected the extreme rain during the Great Famine to the GFM, which for most of the last millennium comprised the leading mode of European hydroclimate variability and is associated with the most extreme summer wet and dry events over Europe, the Great Famine included. For reasons currently unknown, the GFM receded in influence over the 20th century relative to a N–S mode resembling the NAO, holding implications for future hydroclimate extremes should this change be anomalous or temporary.

Methods

We employ the Old-World Drought Atlas[12] (OWDA) to quantify European soil moisture conditions during the Great Famine. The OWDA is a 0.5° gridded tree-ring based reconstruction of soil moisture spanning 1 – 2012 Common Era (C.E.) that estimates boreal summer (June–July–August) self-calibrating Palmer's Drought Severity Index[13] (scPDSI), with persistence from previous months factored into the calculation of monthly scPDSI to reflect more slowly changing soil moisture content[12]. We composite the OWDA over the Great Famine years of 1314–1316 (individually and as a 3-year interval) and rank these wet conditions against the broader paleoclimate record from 1300 to 2012 C.E., using modern nation states as the geographic boundaries for the spatial analyses. The 1300–2012 interval is chosen for consistency of comparison to population estimates for England, France, and Italy, which jointly become available after 1300 (e.g. Alfani and Gráda[14]). We furthermore restrict all analyses of the OWDA to post 1300 due to loss of tree-ring records prior to this time. We perform empirical orthogonal function (EOF) analysis of the OWDA to identify leading modes of hydroclimate variability over the OWDA domain and examine their respective relationships to European scPDSI (defined as "All Countries" in Table 1, which excludes Italy).

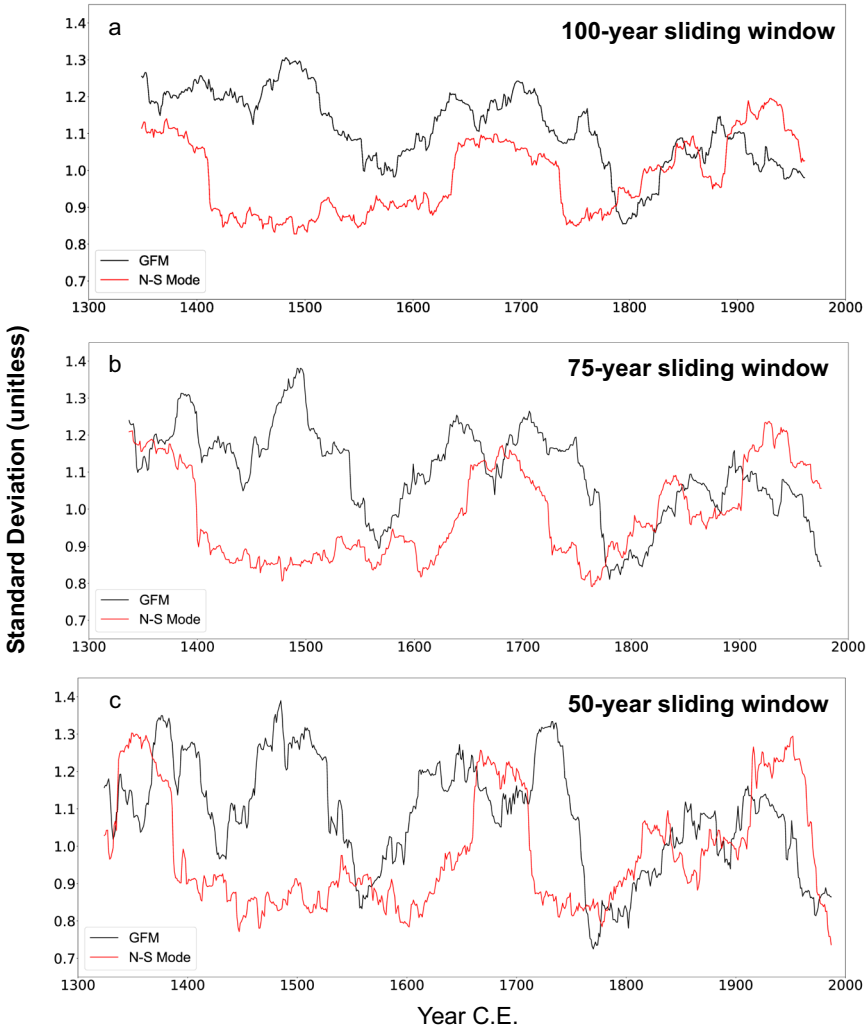

Fig. 4 Principle components of the Great Famine mode. Standard deviations of running **a** 100-year, **b** 75-year, and **c** 50-year windows for the GFM mode (i.e. first leading PC) and the N–S mode (i.e. second leading PC) in the OWDA from 1300 to 2012. The GFM and N–S modes are normalized by the standard deviation of the N–S mode.

We additionally employ monthly precipitation data from the Climatic Research Unit Time-Series version 4.03 product[28], available on a 0.5° grid from 1901 to 2018. We perform EOF analyses to identify the leading modes of precipitation over 1901–2012, then compare their respective patterns to those identified in the OWDA.

Finally, we employ medieval population data (for England and France) and a European famine chronology from Alfani and Gráda[14]. We rank the population of England and France during 1314, 1315, 1316, and 1317 relative to all years from 1300 to 1700 and the subset of famine years during 1300–1700 (years preceding famines for 1314).

Data availability

The OWDA is publicly available at (https://www.ncdc.noaa.gov/paleo-search/study/19419). The famine chronology is available in the Supplementary Information of Alfani and Gráda[14]. The population data for England and France are available at (https://openicpsr.org/openicpsr/project/120551/version/V1/view).

Code availability

All code necessary to perform the reported analyses is available at (10.5281/zenodo.3952638).

Received: 24 March 2020; Accepted: 4 August 2020;
Published online: 15 September 2020

References

1. Green, D. *The Hundred Years War: A People's History* (Yale University Press, New Haven, 2014).
2. Benedictow, O. J. *The Black Death 1346-1353: The Complete History* (The Boydell Press, Woodbridge, 2004).
3. Campbell, B. *The Great Transition: Climate, Disease and Society in the Late-Medieval World* (Cambridge University Press, Cambridge, 2016).
4. Lima, M. Climate change and the population collapse during the "Great Famine" in pre-industrial Europe. *Ecol. Evol.* **4**, 284–291 (2014).
5. Intergovernmental Panel on Climate Change. *Information from Paleoclimate Archives. In Climate Change 2013 – The Physical Science Basis: Working Group I Contribution to the Fifth Assessment Report of the Intergovernmental Panel on Climate Change*, 383–464 (2014).
6. Lucas, H. The Great European Famine of 1315, 1316, and 1317. *Speculum* **5**, 343–377 (1930).
7. Campbell, B. Nature as historical protagonist: environment and society in pre-industrial England. *Econ. Hist. Rev.* **63**, 281–314 (2010).
8. Kershaw, I. The great famine and agrarian crisis in England 1315–1322. *Past & Present* **59**, 3–50 (1973).
9. Erthel, Tim. *Mitteilungen des Vereins für die Geschichte und Altertumskunde von Erfurts*. 70 (Sutton Verlag 2009).
10. Jordan, W. *The Great Famine: Northern Europe in the Early Fourteenth Century* (Princeton University Press 1996).
11. Rosen, W. *The Third Horseman: A Story of Weather, War, and the Famine History Forgot* (Viking Press 2015).

12. Cook, E. R. et al. Old World megadroughts and pluvials during the Common Era. *Sci. Adv.* **1**, e1500561 (2015).
13. van der Schrier, G., Barichivich, J., Briffa, K. R. & Jones, P. D. A scPDSI-based global data set of dry and wet spells for 1901–2009. *J. Geophys. Res. Atmos.* **118**, 4025–4048 (2013).
14. Alfani, G. & Gráda, Ó. C. The timing and causes of famines in Europe. *Nat. Sustain.* **1**, 283–288 (2018).
15. Slavin, P. *Experiencing Famine in Fourteenth-Century Britian* (London, Brepols Publishers, 2019).
16. Pribyl, K. *Farming, Famine and Plague: The Impact of Climate in Late Medieval England* (Springer, Cham, 2017).
17. Markonis, Y. et al. Persistent multi-scale fluctuations shift European hydroclimate to its millennial boundaries. *Nat. Commun.* **9**, 1767 (2018).
18. Baek, S. H. et al. Precipitation, temperature, and teleconnection signals across the combined North American, Monsoon Asia, and old world drought atlases. *J. Clim.* **30**, 7141–7155 (2017).
19. Zveryaev, I. I. & Allan, R. P. Summertime precipitation variability over Europe and its links to atmospheric dynamics and evaporation. *J. Geophys. Res.* **115**, D12102 (2010).
20. Anchukaitis, K. J. et al. Coupled modes of North Atlantic ocean-atmosphere variability and the onset of the Little Ice Age. *Geophys. Res. Lett.* **46**, 12417–12426 (2019).
21. van Loon, H. & Rogers, J. C. The seesaw in winter temperatures between Greenland and northern Europe. Part I: general description. *Mon. Weather Rev.* **106**, 296–310 (1978).
22. Barnston, A. G. & Livezey, R. E. Classification, seasonality and persistence of low-frequency atmospheric circulation patterns. *Mon. Weather Rev.* **115**, 1083–1126 (1987).
23. Rogers, J. C. & van Loon, H. The seesaw in winter temperatures between Greenland and northern Europe. Part II: some oceanic and atmospheric effects in middle and high latitudes. *Mon. Weather Rev.* **107**, 509–519 (1979).
24. Hurrell, J. W. Decadal trends in the North Atlantic Oscillation: regional temperatures and precipitation. *Science* **269**, 676–679 (1995).
25. Hurrell J. W., Kushnir Y., Visbeck M., Ottersen G. in *The North Atlantic Oscillation* (eds. Hurrell J. W., Kushnir Y., Otterson G., Visbeck M. H.) Vol. 134. 1–35 (AGU Geophysical Monograph, New York, 2003).
26. Hurrell, J. W. & Deser, C. North Atlantic climate variability: the role of the North Atlantic Oscillation. *J. Mar. Syst.* **79**, 231–244 (2009).
27. Cook, E. R. et al. A Euro-Mediterranean tree-ring reconstruction of the winter NAO index since 910 C.E. *Clim. Dyn.* **53**, 1567–1580 (2019).
28. University of East Anglia Climatic Research Unit; Harris, I.C., Jones, P.D. *CRU TS4.03: Climatic Research Unit (CRU) Time-Series (TS) version 4.03 of high-resolution gridded data of month-by-month variation in climate (Jan. 1901- Dec. 2018)* (Centre for Environmental Data, 2020).

Acknowledgements

We thank Guido Alfani for providing the population data used in this study. We are grateful to Rhiannon Stephens for her helpful edits and comments on an early draft of the manuscript. This work was supported by the Department of Earth and Environmental Sciences of Columbia University, NSF grant AGS-1734760, and the Lamont-Doherty Earth Observatory summer intern program. LDEO contribution 8440.

Author contributions

J.E.S., E.R.C., B.I.C., R.S., and M.A.C. conceived the study. S.H.B. and J.E.S. designed the study. S.H.B., G.D., and J.G.N. performed the analyses, with contributions from J.E.S., E.R.C., B.I.C., R.S., M.A.C., and S.R.S. in interpreting the results. S.H.B. and J.E.S. wrote the paper, with contributions from all co-authors.

Competing interests

The authors declare no competing interests.

Additional information

Supplementary information is available for this paper at https://doi.org/10.1038/s43247-020-00016-3.

Correspondence and requests for materials should be addressed to S.H.B.

Peer review information Primary handling editor: Joe Aslin.

Reprints and permission information is available at http://www.nature.com/reprints

Publisher's note Springer Nature remains neutral with regard to jurisdictional claims in published maps and institutional affiliations.